

# DESIGN STRATEGY OF THE MULTIFUNCTIONAL WATER SPECIES RETAINED IN VARIOUS FOODS

Yasuyuki Konishi<sup>1\*</sup>, Masayoshi Kobayashi<sup>2</sup>

<sup>1\*</sup>Hokkaido Industrial Technology Center 379 Kikyo-cho, Hakodate, Hokkaido 041-0801, Japan

<sup>2</sup>Advanced Technology Institute of Northern Resources 8-6, Tonden 2Jo 2Chome, Sapporo, Hokkaido 002-0852, Japan

**ABSTRACT:** Multifunctional water species retained in seven foods (squid, sardines, scallops, salmon, beef (produced in Australia and Hokkaido), and pork) were clearly distinguished by using a newly chosen parameter of proton NMR correlation time,  $\tau_C$  (s), as water species-A<sub>1</sub>, water species-A<sub>2</sub>, self-organized water species (SOWS), and non-self-organized water species (NSOWS). A forced cyclic temperature change operation (FCTCO) between 30 and -30°C clearly demonstrated a forced oscillation of the self-organized water species (FOSOW) retained in the seven foods using the  $\tau_C$ . The activation energies for the FOSOW, described as a function of  $1/\tau_C$  (molecular mobility,  $s^{-1}$ ), were quantitatively distinguished based on the variety of water species and the kinds of food. The oscillating modes obtained demonstrated the existence of two different water species regions, -A<sub>1</sub> and -A<sub>2</sub>, which were divided at  $\tau_C = 10^{-8}$  s (=  $C\tau_C$ ). The amplitude ( $\alpha$ ) of the FOSOW for water species-A<sub>1</sub> was larger than that for water species-A<sub>2</sub>. Water species-A<sub>1</sub> was characterized as a weakly restricted species with a higher  $1/\tau_C$  and larger  $\alpha$ , whereas water species-A<sub>2</sub> was recognized as a strongly restricted species with a larger  $\tau_C$  and smaller  $\alpha$ . The probability of self-organization was described by a linear dependency as a function of the amount of self-organized water (ASOW).

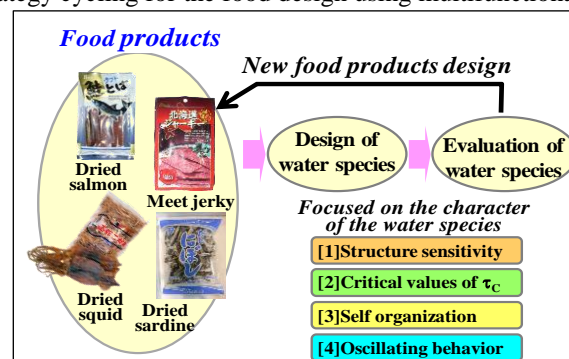
**Keywords:** Molecular mobility, self-organization, hysteresis, water species-A<sub>1</sub> and -A<sub>2</sub>, forced cyclic temperature change operation (FCTCO).

## 1. INTRODUCTION

### 1.1. Strategy Challenging the Design of Multifunctional Water Species

As has been demonstrated in many papers [1-4], the water species retained in various food products are recognized as being multifunctional in nature. In designing the specified characteristics of water species retained in food products, multifunctional water species with the specified parameters of discriminating multifunctional natures have been demonstrated to change dynamically depending on environmental conditions such as temperature, pressure, and humidity. Figure 1 illustrates a challenging cycling strategy for designing food products that exhibit a simplified model description. The food products were repeatedly examined so as to ensure that they achieved the requested tastes.

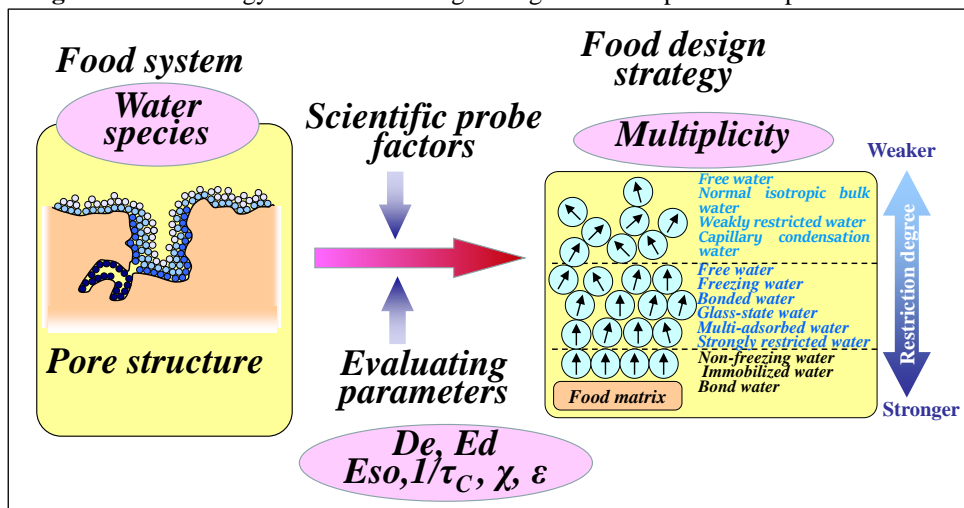
Figure 1. Strategy cycling for the food design using multifunctional water species.



## 1.2. Strategy for Food Product Design Using Water Species as a Probe Molecule

For a concrete demonstration of the multifunctionality of water species, our interests are focused on: (1) the characterization of the structure sensitivity with respect to the physical structure of food solids; (2) the critical value decision derived from the proton NMR correlation time,  $\tau_c$ , distinguishing the kinds of multifunctional water species; (3) the dynamic self-organization behavior: water species retained in foods have specified temperature regions for making their own self-organization behavior as characterized by the given kinds of foods; and (4) oscillating behavior: multifunctional water species might be responding to the dynamic behavior between the non-self-organized and self-organized states derived from the oscillating change in temperature. The self-organization behavior would be characterized by the kind of food products, and the taste of the food products would be sensitively influenced by the specific multifunctional water species. The water species' characteristics integrated from the physio-chemical nature would strongly contribute to increasing food product quality. Figure 2 illustrates a rough representation of the strategy for designing high-quality food products using the water species as a probe molecule [5-9]. One can recognize various specified parameters as scientific probe factors for detecting the multiplicity of water species, as shown in Fig. 2, to understand the food design strategy.

Figure 2. The strategy for the food design using the water species as a probe molecule.



In the present paper, the objectives are (1) to distinguish the variety of water species that vary dynamically depending on environmental conditions as structure sensitivities of food solids, (2) to clearly distinguish the complexity of the multifunctional water species using the proton NMR correlation time ( $\tau_c$ , s) without depending on the kind of food, (3) to characterize both the dynamism of self-organized water species (SOWS) and the response of the forced cyclic temperature change operation (FCTCO) depending on the kind of food, and (4) to visualize the three-dimensional demonstration of self-organization behavior of the water species as characterized by the food products.

## 2. EXPERIMENTAL

Seven kinds of food—salmon, squid, sardine, scallop, beef (produced in Australia,  $B_A$ , and Hokkaido,  $B_H$ ), and pork (produced in Hokkaido,  $P_H$ )—were used as typical examples; all had initial moisture contents of 230~280 %-d.b. (dry basis,  $W_D$ ). Each sample was placed in a stainless-steel net tray (4 mesh) that was mechanically hung from a strain-gauge transducer in the dryer. The sample weight was continuously recorded by the output of the strain-gauge transducer using a data logger. Drying temperatures ( $T_D$ ) of 40, 50, 60, 70, and 80 °C were chosen. The sample weight was continuously recorded by the output of a strain-gauge transducer using a data logger. Under the present experimental drying conditions, it was reconfirmed that the drying operations were within a falling-rate period. The diffusivity ( $De$ ) of a sample at a given moisture content was evaluated by Eqs. (1) and (2) [10-12].

$$\frac{W - W_e}{W_D - W_e} = \left(\frac{8}{\pi^2}\right)^3 \exp\left(\frac{\pi^2 \cdot De \cdot t}{4} \cdot (L_a^{-2} + L_b^{-2} + L_c^{-2})\right) \dots\dots\dots (1)$$

$$De = \left(\frac{\varepsilon}{\chi}\right) \cdot D = \delta \cdot D_0 \cdot \exp\left(\frac{-E_D}{R \cdot (T_D + 273)}\right) \dots\dots\dots (2)$$

where  $W$  is the moisture content (%-d.b.) at the drying time  $t$  (h);  $W_e$  is the equilibrium moisture content (%-d.b.);  $W_D$  is the initial moisture content of a drying fresh sample (%-d.b.);  $t$  is the drying time (h); and  $L_a$ ,  $L_b$ , and  $L_c$  are the half-distances of the sample width (m).  $\varepsilon$  is the volume fraction void in the body of food solids;  $\chi$ , the tortuosity, is a structural factor accounting for increased diffusional path length and varying channel cross section seen by individual diffusin molecules;  $D$  is some intrinsic transport coefficient;  $\delta$  is the diffusibility;  $D_0$  is a frequency factor including  $\delta$ ; and  $E_D$  is the activation energy of diffusion [12].

To discriminate between water species retained in the seven kinds of food, a nuclear magnetic resonance (NMR) technique was effectively applied to measure the molecular mobility ( $1/\tau_c$  as a function of correlation time  $\tau_c$ ) by using the  $^1\text{H-NMR}$  spectra and spin-spin relaxation time of water protons. The  $^1\text{H-NMR}$  spectra were obtained using a JEOL A-500 FT-NMR spectrometer operating at 500 MHz for protons. The observed frequency width was 20 kHz. The  $90^\circ$  pulse width was  $12.5 \mu\text{s}$ , and the number of pulse repetitions was 8. The proton chemical shifts were measured by using a slight amount of water containing deuterium oxide as an external reference. All NMR measurements were performed at  $23.5 \pm 0.5^\circ\text{C}$ . The spin-spin relaxation times were obtained by the spin-locking method, and, from the times obtained, the correlation time of a water proton,  $\tau_c$ , was evaluated.

The forced cyclic temperature change operation (FCTCO) used in this study was conducted in a specified temperature range at which hysteresis behavior appeared due to the self-organization of water species. In the temperature range for hysteresis (the self-organization range), the samples were kept for  $13(\pm 2)$  min at the given temperature, and each temperature-up or -down operation was successively conducted. The holding time at the temperature to evaluate the relaxation time for the NMR technique was included in the cyclic operation time.

The  $T_2$  (spin-spin relaxation time of the water proton(s)) obtained is related to the correlation time ( $\tau_c$ ) by using Eq. (3) [13]:

$$\frac{1}{T_2} = \frac{\gamma^4 \cdot \hbar^2 \cdot I(I+1)}{5r^6} \left( 3\tau_c + \frac{5\tau_c}{1 + \omega_0^2 \cdot \tau_c^2} + \frac{2\tau_c}{1 + 4\omega_0^2 \cdot \tau_c^2} \right) \dots\dots\dots (3)$$

where  $\gamma$  is the gyromagnetic ratio of a proton ( $=2.675 \times 10^8 \text{ rad} \cdot \text{T}^{-1} \cdot \text{s}^{-1}$ ),  $\hbar$  is the modified Planck's constant ( $6.63 \times 10^{-34} \text{ J} \cdot \text{s}$ ),  $I$  is the nuclear-spin quantum number of a water proton ( $=0.5$ ),  $r$  is the proton-proton distance of a water molecule (0.16 nm),  $\omega_0$  is the resonance frequency of NMR ( $=3.14 \times 10^9 \text{ s}^{-1}$ ), and  $\tau_c$  is the correlation time of the water proton(s). From this equation,  $\tau_c$  values at any given  $T_2$  can be evaluated.

The FCTCO was carefully repeated between  $t_1$  and  $t_2$ , and a forced oscillation of  $1/\tau_c$  was then clearly visualized. In the course of the FCTCO, 2 min to increase or decrease the temperature and 13 min to evaluate the  $T_2$  using the NMR equipment were required; thus, a total of 15 min was needed for measurements at each temperature over the course of the hysteresis period. The oscillating curves obtained were demonstrated as a function of the elapsed time, including the 15 min.

The water activity ( $a_w$ ) of samples was measured using an electrolyte resistive measurement cell (Lab Master- $a_w$ , Novasina Co.). The hardness of the samples was measured using a creep tester. Further detailed experimental procedures and the evaluation details of  $De$  have been presented elsewhere [9-15].

### 3. RESULTS AND DISCUSSION

#### 3.1. Strategy for Designing the Structural Sensitivity of Water Species Retained In Food Products

As has been demonstrated in previous papers, the characteristics of water species retained in food products dynamically and sensitively change according to the degree of dehydration. The key parameters for characterizing the multifunctional water species have usually been unrelated to appearance, for example, water activity ( $a_w$ ), water content ( $W_0$  (%-d.b.)), effective diffusivity of water species ( $De$

( $\text{cm}^2/\text{s}$ ), and activation energy ( $E_D$ ,  $\text{kJ}/\text{mol}$ ) of  $De$ . Figure 3 illustrates  $De$  as a function of  $W_0$ , and Figure 4 illustrates  $aw$  as a function of  $W_0$ . On the horizontal line in both figures, the dehydration time was increased along the left-hand side. The results clearly indicate unclear discrimination of water species- $A_1$  and  $-A_2$ . One can recognize that these illustrations are not effective tools for discriminating between multifunctional water species.

Figure 3. Effective moisture diffusivity of  $B_A$ ,  $B_H$  and  $P_H$  as a function of moisture content ( $T_D = 50^\circ\text{C}$ ).

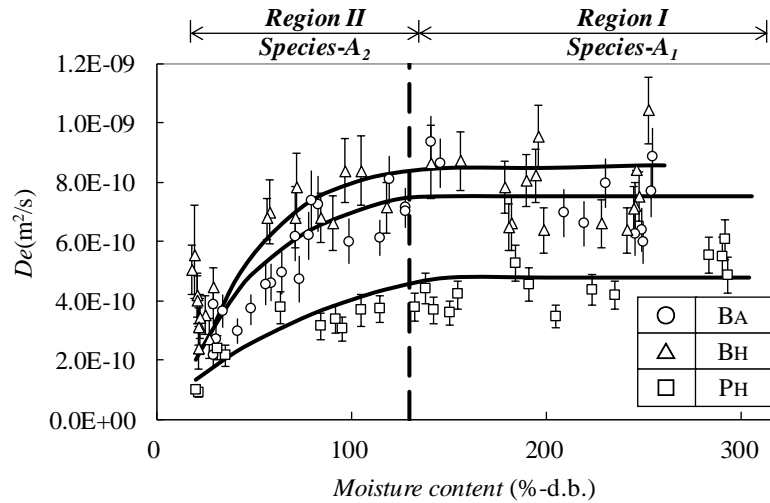
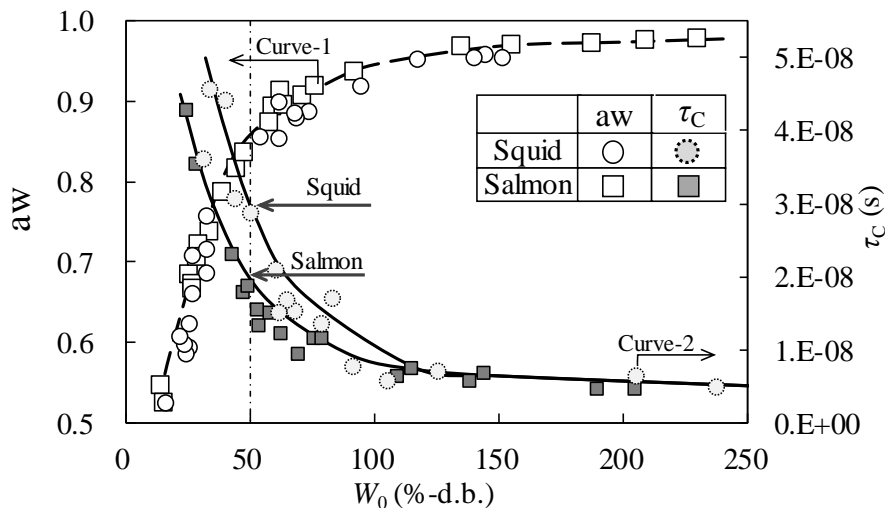


Figure 4.  $aw$  as a function of  $W_0$ .



To overcome this difficulty, Figures 5, 6, and 7 demonstrate a new exhibition tool using three specified parameters—the  $aw$ , the frequency factor of  $De$  ( $\delta D_0$ ), and the hardness,  $N_p$ —as functions of the proton NMR correlation time,  $\tau_c$ . One can clearly recognize that the critical  $\tau_c$ , ( $C\tau_c$ ) demonstrated clear discrimination between water species  $-A_1$  and  $-A_2$ . The boundary value between the two water species gave  $\tau_c = 10^{-8}$  s without depending on the kind of food. One could name the parameter as the critical value of  $\tau_c$  to be  $C\tau_c$ . On the vertical line of Fig. 7, the frequency factor ( $\delta D_0$ ) of  $De$  was calculated by using Eq. (2). The food products were classified into two groups as group-1—for  $B_A$ ,  $B_H$ , and  $P_H$ —and group-2—for squid, salmon, and sardine. The values of  $\delta D_0$  for group-1 were drastically decreased at  $C\tau_c$ , whereas the values for group-2 were increased, indicating their own characteristic pore structures. One could recognize that the change in pore structure induced a drastic change in the three parameters of  $E_D$  and  $N_p$  and the kind of water species from  $-A_1$  to  $-A_2$  at the  $C\tau_c$ . This drastic change of parameters should create the taste characteristics of the food products. Therefore, the  $C\tau_c$  is one of the most important values for characterizing food taste.

Each of the five straight lines in the water species- $A_2$  region of Figure 8 had a different slope, indicating no difference between the two groups. Since the value of  $\delta$  is  $\epsilon/\chi$ , one could recognize that the differences between groups-1 and -2 in Fig. 6 would result from the pore structure changes that were

specifically produced by dehydrating food products. Therefore, water species-A<sub>2</sub> should be characterized by the complicated pore structures of the food products, indicating their own taste identity. Fig. 6 demonstrates the change in hardness ( $N_p$ ) of the foods as a function of  $\tau_c$ . These three change parameters ( $E_D$ ,  $N_p$ , and  $\delta D_0$ ) strongly contribute to the drastic change of the water species from -A<sub>1</sub> to -A<sub>2</sub>.

Although the effective diffusivities presented in Fig. 3 could not be demonstrated for the discrimination of the water species-A<sub>1</sub> and -A<sub>2</sub>, the activation energies ( $E_D$ ) of  $De$  for the three foods ( $P_H$ ,  $B_A$ , and  $B_H$ ) were examined for the clear difference between both species due to the plotting as a function of  $\tau_c$ , as shown in Fig. 5. The results clearly exhibit the drastic reduction of  $E_D$  induced by the drastic change in the pore structure at the  $C\tau_c$ . The change in pore structure contributes to the drastic change of the molecular mobility ( $1/\tau_c$ ) of the water species. In Fig. 6, the hardness of the food products for  $P_H$ ,  $B_A$ , and  $B_H$  clearly demonstrates a drastic increase at the  $C\tau_c$ . Our interest was focused on the reason why the  $C\tau_c$  changed so drastically. The next sections seek to answer that question.

**Figure 5.** Comparing behaviour of  $E_D$  between  $B_A$ ,  $B_H$  and  $P_H$  as a function of  $\tau_c$  at 50~70 °C.

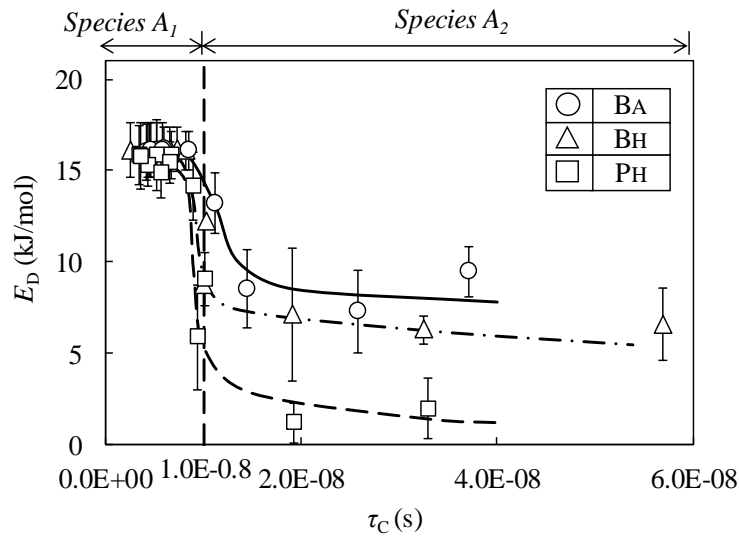


**Figure 6.** Comparing behaviour of  $N_p$  as a function of  $\tau_c$  between  $B_A$ ,  $B_H$  and  $P_H$  at 50 °C.

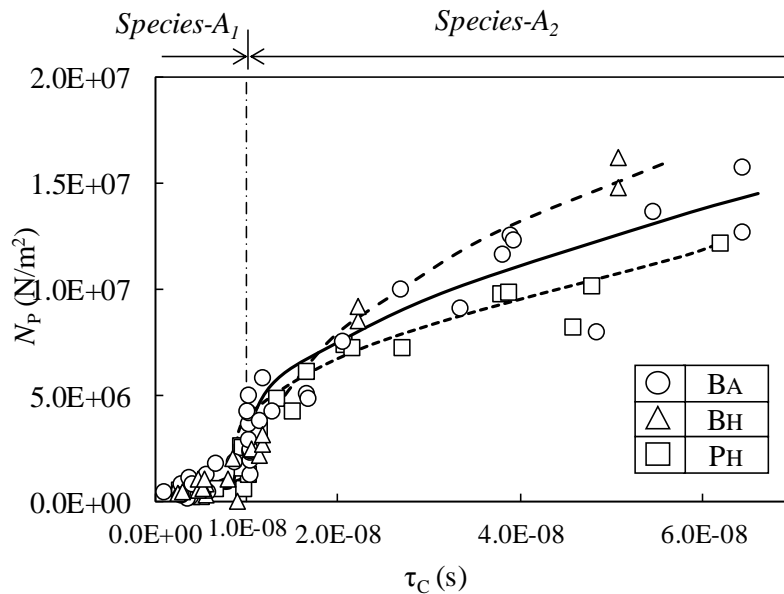
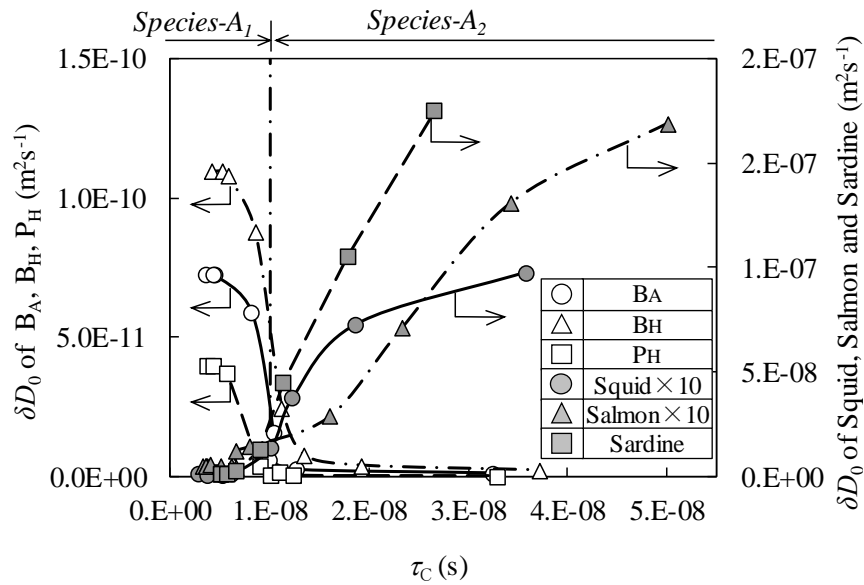


**Figure 7.** Frequency factor of  $De$  as a function of  $\tau_C$ .



Focusing on the slope of the  $aw-\tau_C$  straight line (designated as  $\Delta aw-\tau_C$ ) in Fig. 8, based on our experimental data, we have found much evidence on the different slopes induced by the addition of chemicals into many food products such as salt, saccharides, minerals, and glutamates [14, 15]. These results strongly demonstrate that the  $\Delta aw-\tau_C$  is sensitively influenced by those chemicals and the kinds of food. The  $\Delta aw-\tau_C$  should be an important parameter for determining the taste of the food products, suggesting that multifunctional water species  $-A_1$  and  $-A_2$  are key materials for designing food products. Especially, water species  $-A_2$  could be characterized by the pore structures of food solids contributing to the taste quality. Higher  $\Delta aw-\tau_C$  was ordered as salmon, sardine, squid, and  $B_A$ . This order would be strongly related to the slope of the amount of self-organized water species -  $\tau_C$  straight line ( $\Delta ASOW-\tau_C, \% \cdot d.b. \cdot s^{-1}$ ) which will be presented in a future section (see Fig.18).

Concerning the pore structure change presented in Fig. 7, one could focus on the diffusibility ( $\delta = \epsilon/\chi$ ); the  $\delta$  parameter informs us of the pore structure as imaginatively visualized in Figure 9. The dehydration of food solids causes a drastic change in the pore structure at the  $C\tau_C = 1 \times 10^{-8}$  s to produce water species- $A_2$ . The pore structures thusly produced two different food groups, group-1 ( $P_H, B_A$ , and  $B_H$ ) and group-2 (squid, sardine, and salmon). Group-1 was characterized by the labyrinth factor ( $\chi$ ), becoming large, whereas group-2 became small. In addition, even though the value of the entropy term ( $\Delta S$ ) (which is involved in  $D_0$ ) is difficult to evaluate, the  $\Delta S$  of the pre-exponential factor of  $De$  in group-1 would become small, whereas the  $\Delta S$  of group-2 would become large. These differences would induce a variety of tastes of the water species depending on the kind of food product. Conclusively, one could design a specified water species- $A_2$  that could easily produce the taste characteristics of the food solids by using the parameter of  $\tau_C$  in response to the need.

**Figure 8.**  $aw$  for the water species of  $B_A$ , squid, salmon, and sardine was demonstrated as a function of proton NMR correlation time,  $\tau_C$ .

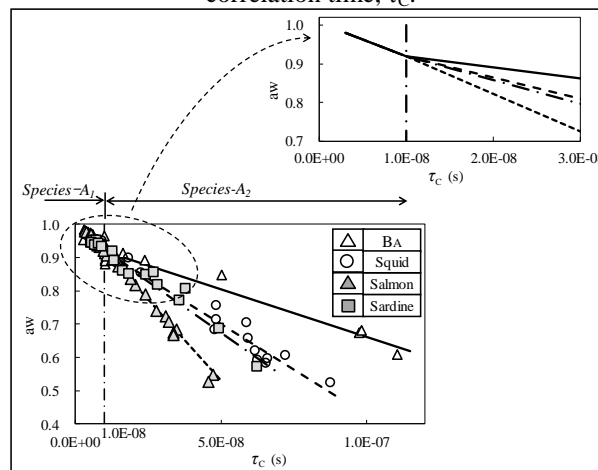
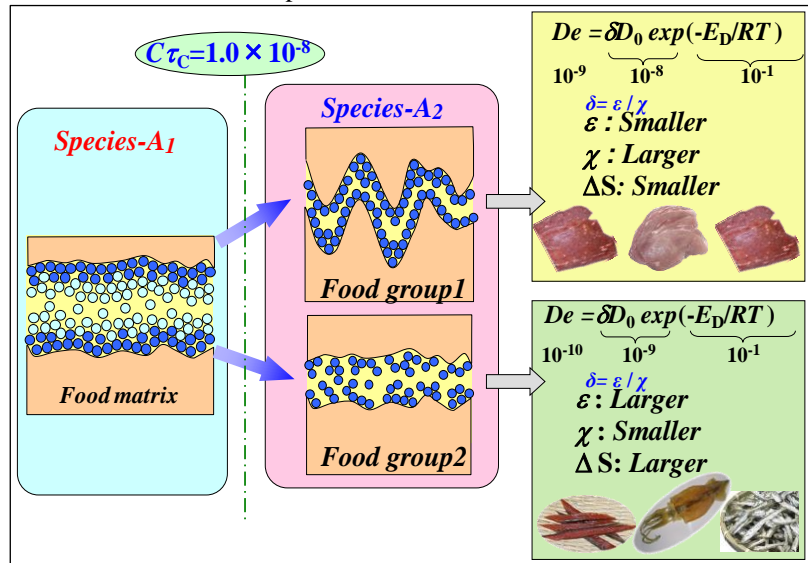
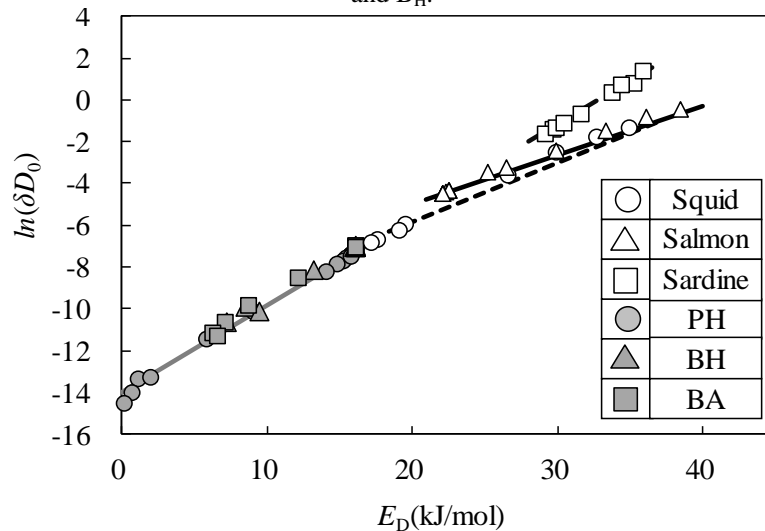


**Figure 9.** Illustrates the dynamic change of the multifunctional water species resulted from the dynamic change of the pore structure of food solid.



Here, our interest was focused on the difference in the diffusion mechanism between the water species retained in the two food groups. To this end, the compensation effect test was examined, as shown in Figure 10. The compensation effect has commonly been used in heterogeneous catalysis reactions as an empirical law. In catalytic reactions, when the reaction would progress on the same sort of active center on the catalyst surface, the number of active centers would be increased to compensate for the increased rate of activation energy. Fig. 10 demonstrates the compensation effect of the test between the pre-exponential factor of  $De$  and the  $E_D$ . One can recognize the two groups—1 and 2—based on their different straight lines. This result strongly demonstrates that the water species retained in food groups -1 and -2 have different diffusion mechanisms, indicating a structure-sensitive characteristic. This structure sensitivity strongly exhibited two different taste characteristics between the two food groups. From this fact, one could have the advantage of being able to design any food flavor by designing the water species.

**Figure 10.** Compensation effect test between the pre-exponential factors and  $E_D$  for squid, salmon, sardine, P<sub>H</sub>, B<sub>A</sub>, and B<sub>H</sub>.



### 3.2. Strategy for Designing the Characteristics of Self-Organized Water Species Using the FCTCO

The dynamic behavior of self-organized water species could be visualized by the forced cyclic temperature change operation (FCTCO), as shown in Figure 11. The temperature was set between room temperature and -35 °C. The proton NMR spectra clearly demonstrated the peak height change of the spectra, as shown in Fig. 11(a). Fig. 11(b) shows the cyclic operation procedure indicating the bottom point at time  $t_1$  and the top point at time  $t_2$ . The peak height is shown as the molecular mobility ( $1/\tau_C$ )

evaluated by using Eq. (3). Fig. 11(c) shows a typical example of the oscillating curves obtained. The amount of self-organized water species (ASOW) could be evaluated from the amplitude of the oscillating curves obtained.

**Figure 11.** Schematic visualization of the forced cyclic-temperature-change operation (FCTCO), the NMR-spectrum dynamism, and the  $1/\tau_C$  oscillation obtained.

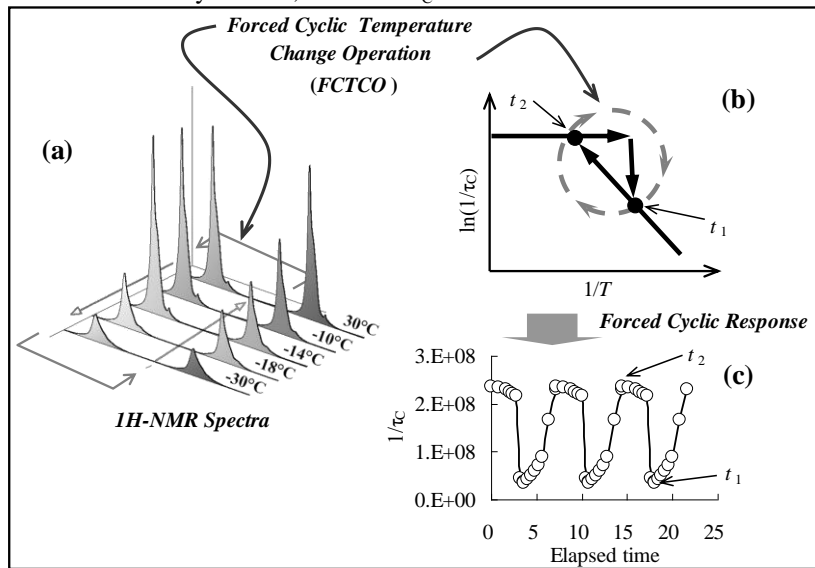
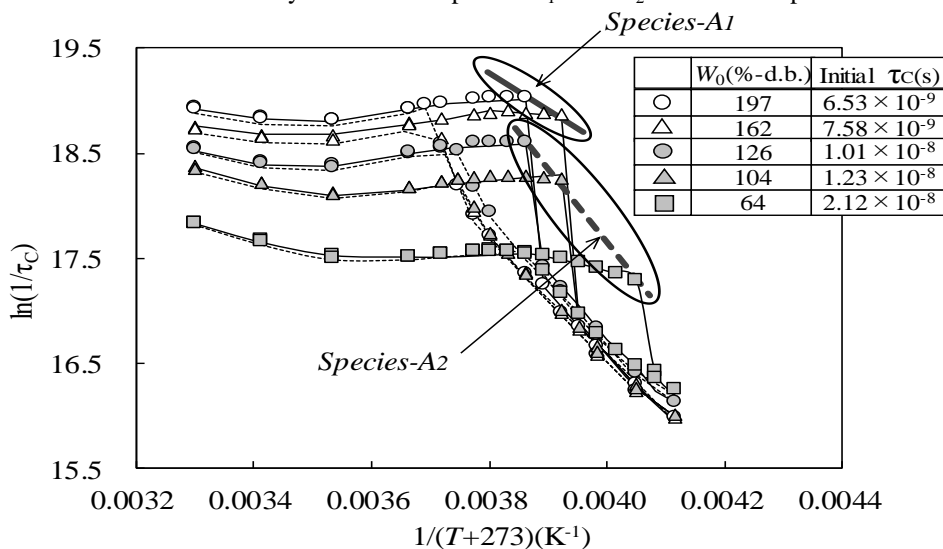


Figure 12 demonstrates typical data for evaluating the activation energy of self-organization using Eq. (4).

$$\frac{1}{\tau_C} = A_{SO} \exp\left(\frac{-E_{SO}}{RT}\right) \dots\dots (4)$$

As shown in Fig. 12, one can recognize a steep reduction in the value of  $\ln(1/\tau_C)$  at the specified  $1/T$  for scallops. From the slopes of the straight lines in Fig. 12, the activation energies for the self-organization of water species-A<sub>1</sub> and -A<sub>2</sub> were evaluated as 29.5 kJ/mol and 58.3 kJ/mol, respectively. The summarized activation energies for the various food products are presented in Table 1. The values of  $E_{SO}$  obtained were widely dispersed depending on both the kinds of water species and food products.

**Figure 12.** The molecular mobility of the water species-A<sub>1</sub> and -A<sub>2</sub> for the scallop as a function of  $1/T$



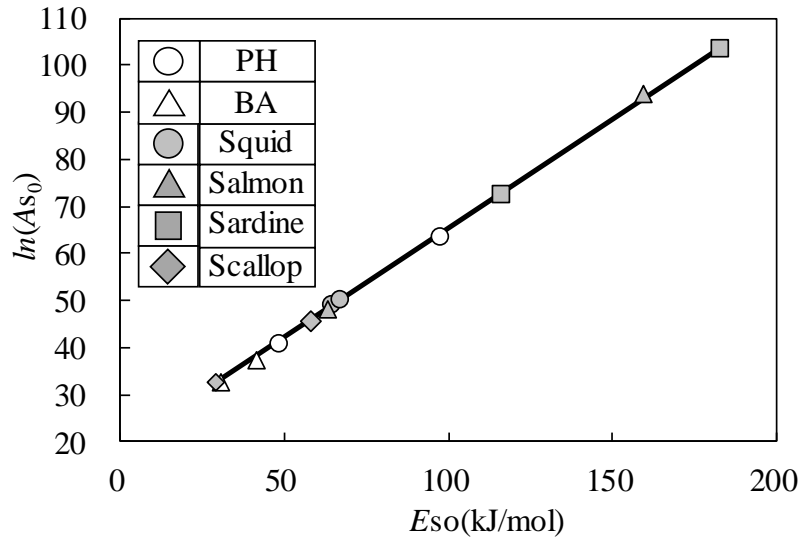
Focusing on the variety of the  $E_D$  values presented in Table 1, one can test the compensation effect of the activation energies for the food products, which was effectively used to test the compensation effect of the pre-exponential factor against the  $E_D$  of  $De$ . Figure 13 clearly demonstrates a good straight line, indicating the

same self-organization mechanism without depending on the kinds of water species and food products. Therefore, self-organized water species should be formed by the same mechanism without depending on both differences in the pore structure and the kind of food product. This means that the self-organization mechanism produces a contrast in the structure insensitivity evident from the structure-sensitive diffusion mechanism of water species derived from the pore-structure change. This result clearly provides interesting evidence because of the double character (dualism) of the water species retained in the food products.

**Table 1.** Activation energies of self-organization for water species-A<sub>1</sub> and - A<sub>2</sub> retained in B<sub>A</sub>, B<sub>H</sub>, P<sub>H</sub>, squid, salmon, sardines, and Scallop.

	$E_{SO}$ (kJ/mol)	
	Species-A <sub>1</sub>	Species-A <sub>2</sub>
B <sub>A</sub>	31	42
P <sub>H</sub>	49	98
Squid	65	67
Salmon	160	63
Sardines	183	116
Scallop	30	58

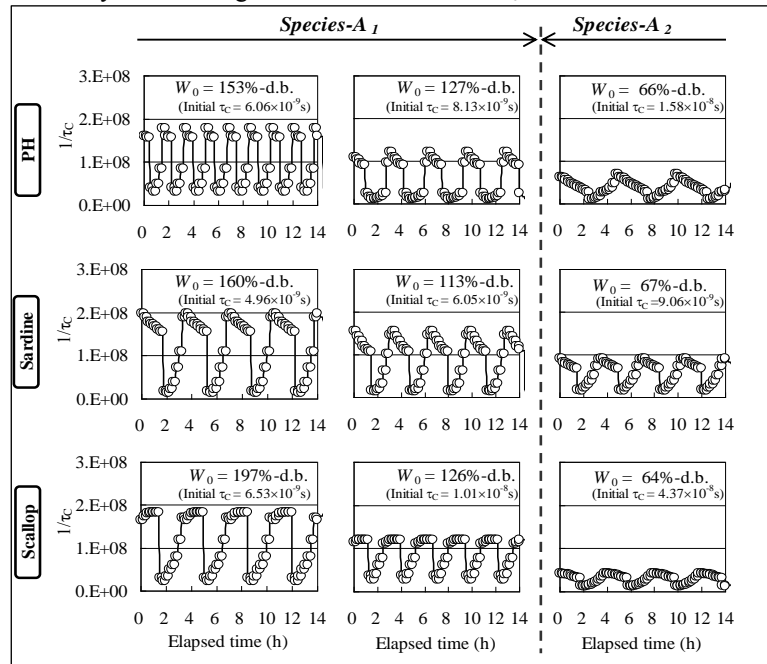
**Figure 13.** Compensation effect between the  $\ln(A_{S_0})$  and  $E_{SO}$  for squid, salmon, sardine, scallop, P<sub>H</sub> and B<sub>A</sub>.



### 3.3. Visualization of the Characteristics of Self-Organized Water Species Derived From FCTCO

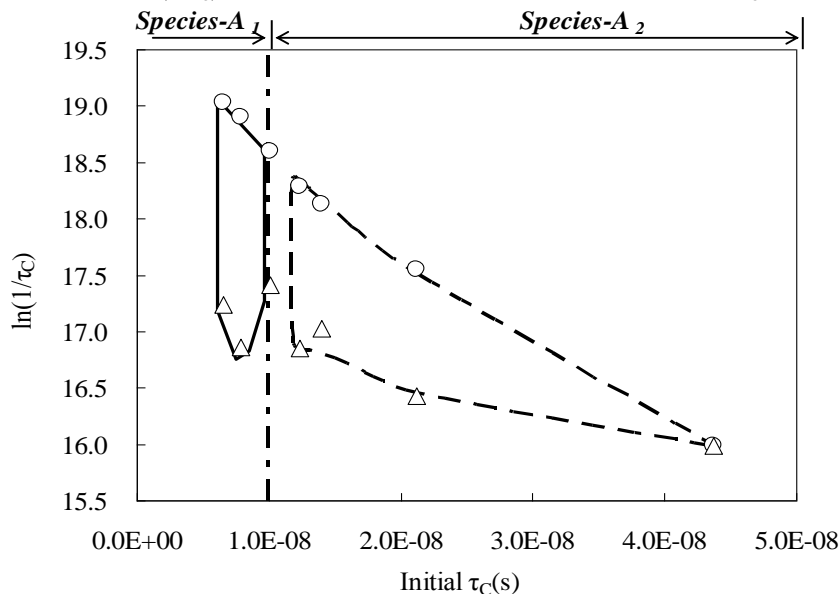
The oscillations of the  $(1/\tau_c)$  values obtained by the forced cyclic temperature change operation (FCTCO) were visualized for all of the foods used in this study. Figure 14 demonstrates the forced oscillating curves for sardines, scallops, and P<sub>H</sub> as typical examples. As is evident in the oscillating response curves obtained, the amplitude ( $A_{S_0}$ ), period, and waveform were characterized depending on the kind of food and the water content (which can be replaced by the initial  $\tau_c$  of the sample).

Figure 14. Dynamic change of  $\alpha$  as a function of  $W_0$  for PH, sardine, and scallop.



When comparing the forced oscillations among the samples, which were widely dispersed by the water contents (or initial  $\tau_c$ 's), as presented in Fig. 14, the amplitude ( $\alpha$ ) of the oscillation was drastically reduced in the water species-A<sub>2</sub> region, indicating a reduction in the molecular mobility ( $1/\tau_c$ ). This reduction of  $\alpha$  in the case of scallops can be recognized easily from the diagram in Fig. 15 by the width of  $\ln(1/\tau_c)$ , which was given as the distance between the peak top and the peak bottom of the oscillating curves in Fig. 14. Figure 15 visualizes the dynamism of the  $\alpha$  as a function of the initial  $\tau_c$ , indicating a broken-line circle, as an example. The width of the broken-line circle decreased steeply with an increase in the initial  $\tau_c$ . Since this decrease means the reduction of the amount of the self-organized water species retained in the food products, the ASOW finally reached zero ( $\alpha = 0$ ) at the specified initial  $\tau_c$ . In this  $\tau_c$  region ( $\tau_c > 4.4 \times 10^{-8}$  s, for scallops), the hysteresis behavior disappeared. Focusing on water species-A<sub>1</sub> and -A<sub>2</sub> regions, the two regions were clearly divided at the critical value of  $C\tau_c = 1 \times 10^{-8}$  s. This was reconfirmed by the comparison of Fig. 16(A) and 16(B). Finally, the  $C\tau_c$  provided a critical boundary for the pore structure change of the food products and the drastic reduction of the ASOW. From these arguments, one can reconfirm that water species-A<sub>1</sub> and -A<sub>2</sub> could be designed by the process of dehydrating food products, indicating the design of food product tastes. This is an important operation for designing the taste of food products.

Figure 15. Width of  $\ln(1/\tau_c)$  for forced oscillation as a function of the initial  $\tau_c$  for the scallops.



**Figure 16.** Correlation between the amount of the self-organized water species and the pore structures of the food product.

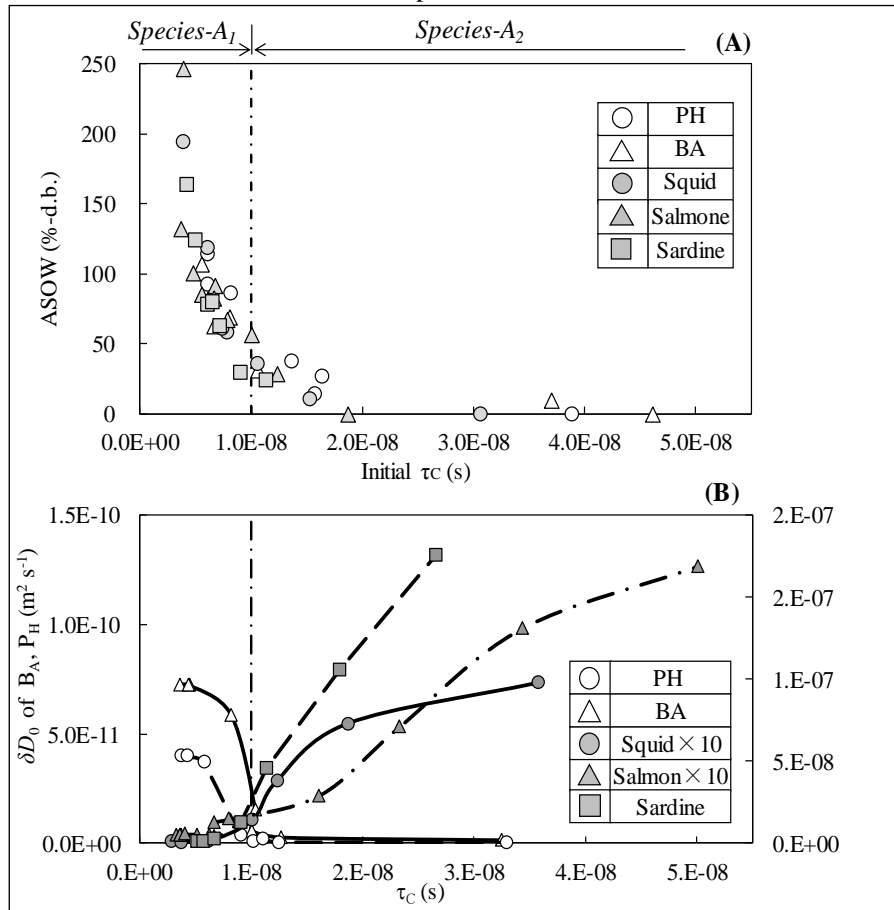
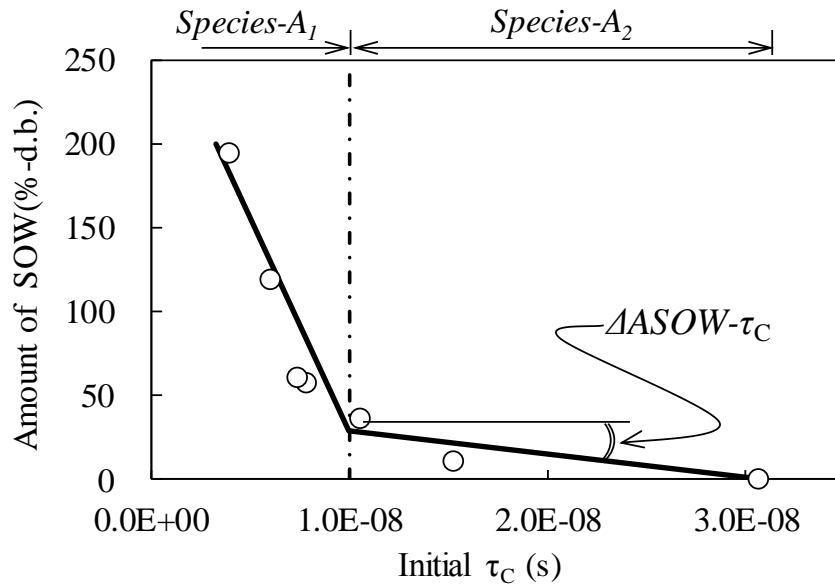


Figure 16(A) illustrates the  $A_{SO}$  as a function of the initial  $\tau_c$ , indicating the disappearance ( $A_{SO} = 0$  %-d.b.) of the oscillation for salmon, squid, P<sub>H</sub>, and B<sub>A</sub> to become the initial  $\tau_c = 1.8 \times 10^{-8}$ ,  $3.0 \times 10^{-8}$ ,  $3.8 \times 10^{-8}$ , and  $4.6 \times 10^{-8}$  s, respectively. These results clearly demonstrate that the water content (corresponding to the initial  $\tau_c$ ) for the disappearance of self-organization was sensitively changed depending on the kind of food. Figure 17 is an illustration of the process of evaluating the possibility of self-organization. In addition, since the slope of each  $A_{SO} \sim \tau_c$  straight line in the species-A<sub>2</sub> region in Fig. 17 produced a specified value depending on the kind of food, one may designate it as an acceleration factor for self-organization, as the slope of the SOW (%-d.b.)  $\sim \tau_c$  (s<sup>-1</sup>) straight line (designated as  $\Delta SOW \sim \tau_c$  (%-d.b.  $\cdot$  s<sup>-1</sup>)). The  $\Delta SOW \sim \tau_c$  value obtained for each food can be used as a parameter for evaluating the degree of acceleration of the self-organization appearance of the water species for a given food, assuming an acceleration parameter. A higher  $\Delta SOW \sim \tau_c$ , therefore, means an easier self-organization disappearance. In Fig. 16(A), the initial  $\tau_c$  to cause the amounts of the SOW to become zero were evaluated as  $1.8 \times 10^{-8}$  s for salmon,  $3.1 \times 10^{-8}$  s for squid,  $3.8 \times 10^{-8}$  s for P<sub>H</sub>, and  $4.6 \times 10^{-8}$  s for B<sub>A</sub>. Therefore, B<sub>A</sub> had a higher probability of self-organization than did P<sub>H</sub> and squid because of the higher slope of the  $\Delta ASOW \sim \tau_c$  line.

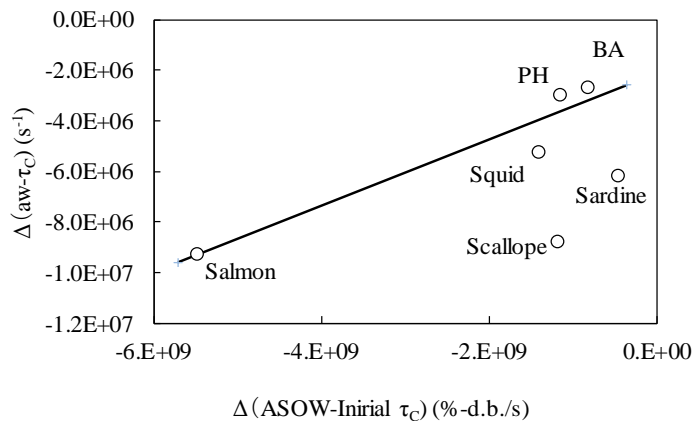
**Figure 17.** Evaluation of the  $\Delta ASOW-\tau_C$  value for the self-organization possibility of the water species



### 3.4. Characteristic Contribution of Water Activity to the Accelerative Possibility for Self-Organization

Concerning the relation between the  $\Delta aw-\tau_C$  presented in Fig. 8 and the initial  $\Delta SOW-\tau_C$  presented in Fig. 18, one could make a characteristic plot. The results are presented in Fig. 18. Although scattered data were recognized, one could presume a rough order as the higher  $\Delta SOW\sim\tau_C$  to be the higher initial  $\Delta SOW-\tau_C$ . This means that the food product  $B_A$  with higher water activity would be retained with higher amounts of self-organized water species ordered as  $B_A$ ,  $P_H$ , squid, and salmon; both the scallop and the sardine deviated from the straight line.

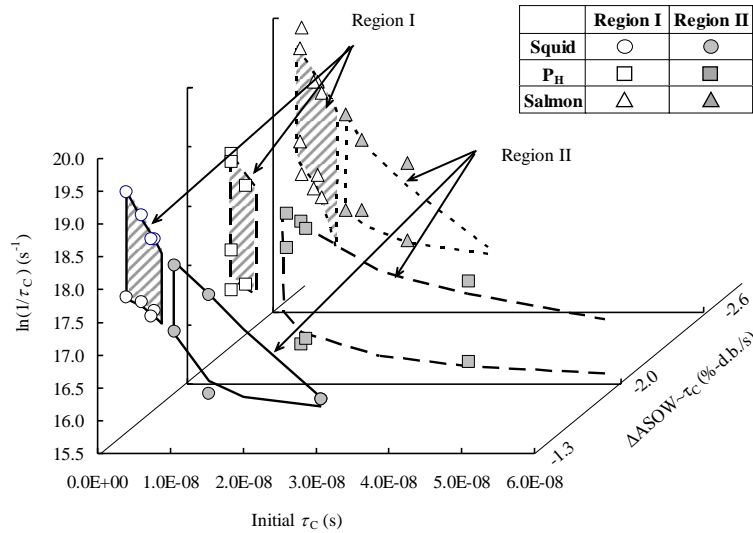
**Figure 18.** The self-organization possibility of the water species as a function of the slope of the ASOW -initial  $\tau_C$  line ( $\Delta ASOW\sim\tau_C$ ).



### 3.5. Visualization of the Three-Dimensional Maps of the Self-Organized Water Species Derived From FCTCO

Figure 19 represents a three-dimensional plot of  $\ln(1/\tau_C)$  [z-axis] as a function of both the initial  $\tau_C$  [y-axis] and the  $\Delta ASOW\sim\tau_C$  [x-axis] for  $P_H$ , squid, and salmon as typical foods. Since the  $\alpha$  is sensitively changed depending on the kind of food, one can recognize a characteristic map mode, as shown in Fig. 19. In the water species- $A_1$  region ( $\tau_C < 10^{-8}$  s, region I), the  $\alpha$  gave an appreciable value without depending on both the initial  $\tau_C$  and the  $\Delta ASOW\sim\tau_C$ , indicating a similarity uninfluenced by the kind of food. On the other hand, in the water species- $A_2$  region ( $\tau_C > 10^{-8}$  s, region II), the mode of the  $Aso$  showed a drastic difference among the foods. The disappearance of the self-organization indicating that  $Aso = 0$ , especially, was given at a different initial  $\tau_C$  value depending on the kind of food, as also seen in Fig. 16(A).

**Figure19.** Three-dimensional visualization of the forced oscillation of the molecular mobility as a function of the  $\Delta ASOW \sim \tau_C$  and the initial  $\tau_C$ .



#### 4. CONCLUSIONS

(1) A forced cyclic temperature change operation (FCTCO) clearly demonstrated the forced oscillating behavior of the water proton's molecular mobility ( $1/\tau_C$ ) because of the self-organization of the multifunctional water species and distinguished between the two water species,  $-A_1$  and  $-A_2$ , retained in the foods, indicating the boundary value of the  $C\tau_C = 1.0 \times 10^{-8}$  s.

(2) The  $C\tau_C$  exactly demonstrated that the foods used were classified into two food groups—1 and 2—which were induced by differences in pore structure. The diffusion mechanism of the two groups of water species produced structure sensitivity, whereas the self-organization mechanism exhibited structure insensitivity. This unexpected result strongly demonstrated a dualism of multifunctional water species- $A_1$  and  $-A_2$ .

(3) The order of the probability for the appearance of self-organization of water species was evaluated as  $B_A > P_H > \text{squid} > \text{salmon}$ , even though the scallop and sardine deviated from the line.

(4) The three-dimensional map of the self-organized water species was visualized by distinguishing the characteristics of the variety of foods used, indicating the variety of the taste.

#### 5. NOMENCLATURES

- $A_1$  weakly restricted water species (-)
- $A_2$  strongly restricted water species (-)
- ANSOWS amount of the non self-organized water species (%-d.b.)
- $A_{SO}$  pre-exponential factor of eq. (4) ( $s^{-1}$ )
- ASOWS amount of the self-organized water species (%-d.b.)
- $\Delta ASOW \sim \tau_C$  slope of the ASOWS -initial  $\tau_C$  straight line (%-d.b. $\cdot s^{-1}$ )
- $\Delta aw - \tau_C$  slope of the water activity -  $\tau_C$  straight line ( $s^{-1}$ )
- $B_A$  beef meat produced in Australia (-)
- $B_H$  beef meat produced in Hokkaido, Japan (-)
- $C\tau_C$  critical correlation time of water proton (s)
- $D$  moisture diffusion coefficient ( $m^2/h$ )
- $D_0$  frequency factor of  $D$  ( $m^2/h$ )
- $De$  effective water diffusion coefficient ( $m^2/h$ )
- $De^0$  pre-exponential factor of  $De$  ( $PF = \delta \cdot D_0$ ,  $m^2/h$ )
- $E_D$  activation energy of water diffusivity (kJ/mol)
- FCTCO forced cyclic temperature change operation (-)
- $I$  nuclear spin quantum number of water proton ( $= 0.5$ ) (--)
- $L_a$  half distance of a-axis of the rectangular sample (m)
- $L_b$  half distance of b-axis of the rectangular sample (m)
- $L_c$  half distance of c-axis of the rectangular sample (m)

$N_P$	hardness of meat products ( $N/m^2$ )
$P_H$	pork meat produced in Hokkaido, Japan (-)
$R$	gas constant ( $= 8.314J/K\cdot mol$ )
$R$	proton-proton distance of water molecule ( $= 0.16\text{ nm}$ )
Region-I	water species- $A_1$ region (-)
Region-II	water species- $A_2$ region (-)
$\Delta S$	activation entropy ( $kJ/mol$ )
$T$	temperature ( $^{\circ}K$ )
$T_2$	spin-spin relaxation time of water proton ( $s$ )
$T_D$	drying temperature ( $^{\circ}C$ )
$t$	drying time ( $h$ )
$ts$	spin locking pulse length( $s$ )
$W$	water content at the drying time $t$ (%-d.b.)
$W_0$	initial water content at the time of PUP operated (%-d.b.)
$W_D$	initial water content of drying flesh sample (%-d.b.)
$W_e$	equilibrium water content (%-d.b.)

## Greek letters

$A$	amplitude of the molecular mobility oscillation induced by the forced cyclic temperature change operation ( $s^{-1}$ )
$\varepsilon$	porosity of the food tissue (-)
$\pi$	the ratio of the circumference of a circle to its diameter ( $=3.14$ )
$\gamma$	gyromagnetic ratio of proton ( $=2.675\times 10^8\text{ rad}\cdot T^{-1}\cdot s^{-1}$ )
$\hbar$	modified Plank's constant ( $=6.63\times 10^{-34}\text{ J}\cdot s$ )
$\omega_0$	resonance frequency ( $=3.14\times 10^9\text{ s}^{-1}$ )
$\tau_c$	correlation time of water proton ( $s$ )
$\chi$	labyrinth factor of the meat tissue (-)
$\delta$	diffusibility ( $=\varepsilon/\chi$ ) (-)

## ACKNOWLEDGEMENT

The authors wish to thank associate professor Koichi Miura, Kitami Institute of Technology, for his effective assistance with the proton NMR analysis.

## REFERENCES

- [1] L. B. Rockland and G. F. Stewart, "International symposium on properties of water, water activity: Influences on food quality, Academic Press Inc., London,," 1981.
- [2] S. J. Schmidt, "Water and solids mobility in foods, Advances in food and nutrition research, volume 48, pp.1-101, Edited by S. L. Talor, Elsevier," 2004.
- [3] O. Fennema, "In principles of food science, Part 1, Marcel Dekker, New York," 1976.
- [4] Y. Konishi and M. Kobayashi, "Challenging evaluation of the hybrid technique of chemical engineering-proton NMR technique for food engineering, Advances in Chemical Engineering, Ed. Z. Nawz and S. Naveed., pp69-92, published by InTech., Croatia," 2012.
- [5] H. Uedaira, "The Dynamic State of Water in Living System, Jap. J. Surg. Metab. Nutr," vol. 16, pp. 1-9, 1982.
- [6] A. Ohsaka, K. Yoshikawa, and W. Uedaira, "NMR Medical science- Basis and Application, Maruzen, Tokyo," 1984.
- [7] Y. Konishi, M. Kobayashi, and K. Miura, "Characterization of water species revealed in the drying operation of *Todarodes pacificus* Steenstrup using water proton NMR analysis," *International Journal of Food Science and Technology*, vol. 45, pp. 1889-1894, 2010.
- [8] Y. Konishi and M. Kobayashi, "Visualized Characterization of Molecular Mobility for Water Species in Foods," *World Academy of Science Engineering and Technology*, vol. 64, pp. 1169-1174, 2012.
- [9] Y. Konishi and M. Kobayashi, "Quantitative evaluation of the design parameters requested in beef and pork drying operation, AIDIC Conference Series," vol. 9, pp. 177-186, 2009.

- [10] Y. Konishi, J. Horiuchi, and M. Kobayashi, "Dynamic evaluation of the dehydration response curves of food characterized by a poultice-up process using a fish-paste sausage - II. A new tank model for a computer simulation," *Drying Technology*, vol. 19, pp. 1271-1285, 2001.
- [11] Y. Konishi, J. Horiuchi, and M. Kobayashi, "Dynamic evaluation of the dehydration response curves of food characterized by a poultice-up process using a fish-paste sausage - I. Determination of the mechanisms for moisture transfer," *Drying Technology*, vol. 19, pp. 1253-1269, 2001.
- [12] J. B. Butt, "Reaction Kinetics and Reactor Design, prentice-Hall, Inc., Englewood Cliffs, New Jersey 07632," 1980.
- [13] A. Abragam, "The Principles of Nuclear Magnetism, Oxford at the Clarend Press," pp. 347-349, 1963.
- [14] Y. Hirata, K. Miura, H. Matsuda, Y. Konishi, and M. Kobayashi, "Meaning of the Proton NMR correlation time for the taste cooking of food products, Regional Meeting of the Chemical Engineering Conference of Japan," 2015.
- [15] K. Miura, K. Matsuda, Y. Konishi, E. Kidokuchi, and M. Kobayashi, "Seasoning design due to the water species retained in foods," in *Regional Meeting of the Chemical Engineering Conference of Japan*, 2012.